Ligand Binding Energies in Cationic Platinum(II) Complexes: A Quantitative Study in the Gas Phase

Marc-Etienne Moret and Peter Chen*

Laboratorium für Organische Chemie, Eidgenössische Technische Hochschule Zürich (ETHZ), Zürich, Switzerland

Received October 31, 2006

Quantitative energy-resolved reactive cross-section measurements and DFT calculations are used to investigate the binding energies of various ligands to the metal center in cationic Pt(II) diimine complexes involved in C−H activation reactions. Independent synthesis of isomeric ions establishes the structure of the adducts formed in gas-phase reactions. The order and relative magnitude of a series of ligand binding energies extracted from experimental cross-sections reproduce the trends seen in solution-phase experiments only when the proper transition state model is employed in the deconvolution of the experimental cross-sections. The choice of transition state model can be rationalized by qualitative structural arguments as well as quantum chemical calculations of the reaction coordinate for the dissociation of the range of possible ligands.

Introduction

The development of efficient catalytic transformations of alkanes is one of the most prominent challenges for today's organometallic chemists, due to both the difficulty of functionalizing relatively inert C−H bonds and the appealing industrial perspectives it would open, such as the use of methane and simple alkanes and arenes as chemical feedstock.[1] Following the early work of Shilov[2] and Garnett,[3] C−H activation by platinum(II) complexes was extensively studied with respect to both mechanism[4] and applications.[5] In particular, cationic complexes incorporating chelating diimine ligands have been found[6,7] to activate both methane and benzene under mild conditions as shown in Scheme 1.

The mechanism of this reaction has been addressed by means of NMR,[6,8−10] UV−vis,[10,11] and mass spectroscopic methods.[11] Recently, we reported a quantitative study of ligand binding energies to the $[(N-N)PtCH_3]^+$ fragment by energy-resolved reactive cross-section measurements of the ions of interest.[12] Given that both solution-phase and gas-phase studies of the C−H activation of benzene and methane by Pt(II) diimine complexes find that ligand exchange is rate-limiting, one can argue that a careful characterization of this step is a major component in the further understanding, development, and optimization of C−H activation chemistry. Extending the range of ligands in our gas-phase thermochemical experiments from the coordinating solvents, acetonitrile, water, and 2,2,2-trifluoroethanol (TFE), to hydrocarbon substrates, benzene, in particular, we observed what appeared at first to be a thermochemical anomaly, which raised two questions: (i) What is the structure of the gas-phase adduct prepared by reaction of $[(N-N)PtCH_3]^+$ and benzene? (ii) Do the ligand dissociations proceed by structurally similar transition states for all of the potential ligands? Addressing these two questions, we present a quantitative study of the potential energy surface (PES) of the ligand dissociation step in the C−H activation reaction in the gas phase, based on both experimental and computational methods.

Scheme 1. C−H Activation Reaction by Diimine Pt(II) Complexes[a]

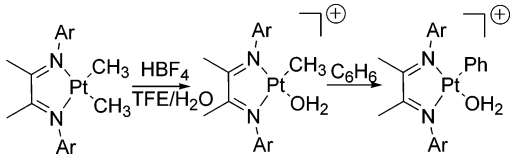

[a] In this study, Ar = 2,6-dichlorophenyl.

Experimental Section

General Procedures. Diethyl ether was distilled from Na/K alloy, dichloromethane from CaH_2, and 1,1,1-trifluoroethanol (TFE) from $MgSO_4$ and $NaHCO_3$, all under a dry nitrogen atmosphere. All chemical manipulations involving platinum complexes were performed under an inert atmosphere using standard Schlenk and glovebox techniques unless otherwise stated. ^1H and ^{13}C NMR spectra were recorded on Varian Gemini 300, Varian Mercury 300, and Bruker ARX 300 instruments. ^1H and ^{13}C chemical shifts are reported in ppm relative to tetramethylsilane, using the residual solvent proton resonance as internal standard. Elemental analyses were carried out by the Mikrolabor of the Laboratorium für Organische Chemie of ETH Zürich. ArNC(Me)C(Me)NAr (Ar = 2,6-dichlorophenyl) (**6**) and the corresponding $(N-N)Pt(CH_3)_2$ complex were prepared as described previously.[11] A mixture of *cis*- and *trans*-$PtCl_2(SMe_2)_2$ was synthesized by a modification of

* Corresponding author. E-mail: chen@org.chem.ethz.ch.

(1) Labinger, J. A.; Bercaw, J. E. *Nature* **2002**, *417*, 507.
(2) Shilov, A. E.; Shul'pin, G. B. *Chem. Rev.* **1997**, *97*, 2879.
(3) Garnett, J. L.; Hodges, R. J. *J. Am. Chem. Soc.* **1967**, *89*, 4546.
(4) Lersch, M.; Tilset, M. *Chem. Rev.* **2005**, *105*, 2471.
(5) Periana, R. A.; Bhalla, G.; W. J. T., III; Young, K. J. H.; Liu, X. Y.; Mironov, O.; Jones, C. J.; Ziatdinov, V. R. *J. Mol. Catal. A* **2004**, *220*, 7.
(6) Heiberg, H.; Johansson, L.; Gropen, O.; Ryan, O. B.; Swang, O.; Tilset, M. *J. Am. Chem. Soc.* **2000**, *122*, 10831.
(7) Johannsson, L.; Ryan, O. B.; Tilset, M. *J. Am. Chem. Soc.* **1999**, *121*, 1974.
(8) Wik, B. J.; Lersch, M.; Krivokapic, A.; Tilset, M. *J. Am. Chem. Soc.* **2006**, *128*, 2682.
(9) Zhong, H. A.; Labinger, J. A.; Bercaw, J. E. *J. Am. Chem. Soc.* **2002**, *124*, 1378.
(10) Johansson, L.; Tilset, M.; Labinger, J. A.; Bercaw, J. E. *J. Am. Chem. Soc.* **2000**, *122*, 10846.
(11) Gerdes, G.; Chen, P. *Organometallics* **2003**, *22*, 2217.
(12) Hammad, L. A.; Gerdes, G.; Chen, P. *Organometallics* **2005**, *24*, 1907.

10.1021/om0610039 CCC: $37.00
Publication on Web 02/16/2007

a literature procedure.[13] All the other chemicals were obtained commercially and used as received unless otherwise stated.

Complex Syntheses. [(N−N)Pt(CH$_3$)(TFE)]$^+$[BF$_4$]$^-$, ∼5 mM Solution. One droplet of HBF$_4$·Et$_2$O was added to a suspension of (N−N)Pt(CH$_3$)$_2$ (6 mg, 10 μmol) in TFE, resulting in complete dissolution and a color change from violet to orange, and the mixture was stirred for 10 min. The solution was used without further purification for electrospraying **1a**.

[(N−N)Pt(C$_6$H$_5$)(TFE)]$^+$[BF$_4$]$^-$, ∼4 mM Solution. Benzene (0.5 mL, 0.44 g, 5.6 mmol) was added to 2 mL of a $\sim 5 \times 10^{-3}$ M solution of [(N−N)Pt(CH$_3$)(TFE)]$^+$[BF$_4$]$^-$ and stirred for 2 h. The solution was used without further purification for electrospraying **2a** and **2b**.

[(N−N)Pt(C$_2$H$_5$)(TFE)]$^+$[BF$_4$]$^-$, ∼5 mM Solution. One droplet of HBF$_4$·Et$_2$O was added to a suspension of (N−N)Pt(C$_2$H$_5$)$_2$ (**7**; 6 mg, 10 μmol) in TFE, resulting in complete dissolution and a color change from violet to orange, and the mixture was stirred for 10 min. The solution was used without further purification for electrospraying **3a** and **4**.

***cis/trans*-PtCl$_2$(SMe$_2$)$_2$.** (This reaction does not require an inert atmosphere.) To a solution of H$_2$PtCl$_6$·*x*H$_2$O (10.8 g, 22 mmol) in 50 mL of water was added solid N$_2$H$_4$·2HCl (1.16 g, 11 mmol) in small amounts. The flask containing the dark red solution was then placed in a 100 °C bath until no more gas evolution was observed (0.5 h). After cooling to room temperature, a small amount of platinum black was filtered off, 12 mL (0.16 mol) of dimethyl sulfide was added, and the pink suspension was heated to 80 °C until it had completely turned yellow. After cooling, it was extracted with dichloromethane (3 × 50 mL) and the combined organic phases were dried over anhydrous magnesium sulfate. Evaporation of the solvent under reduced pressure yielded the product as a yellow crystalline solid (8.40 g, 97%). ^{1}H NMR (CDCl$_3$, 300 MHz): δ 2.58 (s, $^3J(^{195}\text{Pt}-\text{H}) = 49$ Hz, S*Me*$_2$(*cis*)), δ 2.47 (s, $^3J(^{195}\text{Pt}-\text{H}) = 42$ Hz, S*Me*$_2$(*trans*)), *cis/trans* ratio 1:2.

Pt$_2$(C$_2$H$_5$)$_4$(μ-Me$_2$S)$_2$ (5). A 6.3 mL amount of a 0.46 M solution of ethyllithium in 9:1 benzene/cyclohexane (2.90 mmol) was added to a suspension of finely powdered [PtCl$_2$(Me$_2$S)$_2$] (500 mg, 1.37 mmol) in diethyl ether (20 mL) at −15 °C (ice/salt mixture). The mixture was stirred for 40 min, during which time the yellow solid disappeared, the liquid phase became dark brown, and a white solid (presumably LiCl) appeared. (All workup was performed at 0 °C under argon.) The reaction was quenched with a N$_2$-flushed, cooled (0 °C) dilution of 1 mL of saturated NH$_4$Cl in 20 mL of water. A dark solid was filtered off, then the phases were separated, and the aqueous phase was extracted with 3 × 10 mL of diethyl ether. The combined organic phases were dried over MgSO$_4$, activated charcoal (ca. 0.2 g) was added, and the black mixture was filtered to give a pale yellow solution, which was generally concentrated to about 20 mL and used without further purification. (Evaporation of the solvent *in vacuo* at 0 °C yielded a tan solid that started turning brown as it was becoming dry, as well as when it was allowed to warm to room temperature.) The yield could be estimated from the integrals of the ^{1}H NMR spectrum of a sample taken from the subsequent ligand exchange reaction to 0.20 mmol (29%). ^{1}H NMR (C$_6$D$_6$): δ 2.10 (s, $^3J(^{195}\text{Pt}-\text{H}) = 17$ Hz, 12H, SC*H*$_3$), δ 1.62 (q, $^3J(\text{H}-\text{H}) = 8$ Hz, $^2J(^{195}\text{Pt}-\text{H}) = 93$ Hz, 8H, PtC*H*$_2$CH$_3$), δ 1.38 (t, $^3J(\text{H}-\text{H}) = 8$ Hz, $^4J(^{195}\text{Pt}-\text{H}) = 93$ Hz, 12H, PtCH$_2$*CH*$_3$).

(N−N)Pt(C$_2$H$_5$)$_2$ ((N−N) = ArNC(Me)C(Me)N)Ar, Ar = 2,6-dichlorophenyl) (7). A 225 mg (0.60 mmol) amount of ArNC(Me)C(Me)N)Ar (Ar = 2,6-dichlorophenyl) (**6**) was added to a solution of 0.20 mmol of **5** in 20 mL of ether at 0 °C. The yellow solution was allowed to warm at room temperature and stirred for 4.5 h. (The workup was effected under an argon atmosphere.) The solvent was removed *in vacuo*, the dark green residue was dissolved in 4 mL of dichloromethane at 0 °C, a small amount of black solid (presumably elemental Pt) was removed by filtration, and 12 mL of hexane was slowly added at 0 °C. The solution was left at −20 °C overnight. Subsequent filtration and washing of the solid with hexane (2 × 2 mL), followed by a second crystallization from CH$_2$Cl$_2$/hexane, afforded the product as black microcrystals (92 mg, 37%). On some occasions, separation of the complex from the free ligand by crystallization was not successful, and the product was purified by column chromatography over dry, degassed neutral alumina (30 g) with 1:1 hexane/Et$_2$O as eluant, resulting in pure product but lower yield (43 mg, 17%). The solid product can be handled for short periods under air, but should be stored at 4 °C under an inert atmosphere. Its solutions decompose over several hours when exposed to air or at room temperature, yielding a black precipitate (presumably elemental Pt). Mp: ≥137 °C (dec). ^{1}H NMR (CD$_2$Cl$_2$): δ 7.55 (d, $^3J(\text{H}-\text{H}) = 8$ Hz, 4H, ArH$_m$), δ 7.27 (t, $^3J(\text{H}-\text{H}) = 8$ Hz, 2H, ArH$_p$), δ 1.89 (q, $^3J(\text{H}-\text{H}) = 8$ Hz, $^2J(^{195}\text{Pt}-\text{H}) = 96$ Hz, 4H, PtC*H*$_2$CH$_3$), δ 1.063 (s, 6H, NC(C*H*$_3$)C), δ 0.61 (t, $^3J(\text{H}-\text{H}) = 8$ Hz, $^4J(^{195}\text{Pt}-\text{H}) = 84$ Hz, 6H, PtCH$_2$C*H*$_3$). ^{13}C NMR (CD$_2$Cl$_2$): δ 172.9 (*C*=N), δ 143.4 (C$_{ipso}$), δ 128.7 (C$_{meta}$), 127.8 (C$_{para}$), 127.6 (C$_{ortho}$), δ 21.5 (PtCH$_2$CH$_3$), δ 17.5 (NC(*C*H$_3$)C(*C*H$_3$)N), δ 0.8 (Pt*C*H$_2$CH$_3$), no J(Pt−C) observed. Anal. Calcd for C$_{20}$H$_{22}$N$_2$Cl$_4$Pt: C, 38.29, H, 3.53, N, 4,47. Found: C, 38.34, H, 3.82, N, 4.62.

[(N−N)Pt(C$_2$H$_5$)(CD$_3$CN)]$^+$[BF$_4$]$^-$ Solution. A 50 μL sample of a dilution of HBF$_4$ (50% in water, 19 μL, 0.3 mmol) in TFE-d_3 (1 g) was added to a suspension of **7** (6.3 mg, 10 μmol) in TFE-d_3 (1 g), resulting in complete dissolution and a color change from violet to orange. The mixture was stirred for 10 min, and 50 μL of CD$_3$CN was added. ^{1}H NMR: δ 7.59−7.65 (m,4H, ArH$_m$), δ 7.36−7.45 (m, 2H, ArH$_p$), δ 2.07 (s, 3H, NC(C*H*$_3$)C), δ 1.96 (s, 3H, NC(C*H*$_3$)C, other side), δ 1.37 (q, $^3J(\text{H}-\text{H}) = 7.5$ Hz, $^2J(^{195}\text{Pt}-\text{H}) = 85$ Hz, 2H, PtC*H*$_2$CH$_3$), δ 0.51 (t, $^3J(\text{H}-\text{H}) = 7.5$ Hz, $^4J(^{195}\text{Pt}-\text{H}) = 36$ Hz, 3H, PtCH$_2$C*H*$_3$).

Mass Spectrometry. Mass spectrometric measurements were performed on a TSQ 700 instrument, modified as previously described.[12] The complexes **1a**−**3a** and **2b** were electrosprayed from (1−2) × 10^{-5} M solutions in TFE and 1:4 mixtures of TFE and H$_2$O or pure H$_2$O respectively.

Energy-resolved reactive cross-section measurements were executed as reported earlier.[12] The ions were thermalized in the first 24-pole region to a temperature of 343 K using argon or a suitable reaction gas (3−10 mTorr) and then mass selected by the first quadrupole. They were then reacted with argon in the octopole collision cell while monitoring the products as a function of collision energy. Argon was chosen as reaction gas because it allows working at higher energies in the lab frame in order to move the CID threshold region away from the region where the ion beam is truncated.

The "daughter" mode was used for mass selection, and a retarding potential measurement of the kinetic energy distribution of the ions was performed before each experiment, yielding roughly Gaussian distributions with a fwhm between 1.5 and 2.1 eV in the laboratory frame. The parent and daughter channels were monitored alternately while the collision offset was scanned. Additionally, for each measurement, a normal mass scan was performed with a fixed collision offset to check the gross reaction chemistry and ensure that no unexpected products appeared. The intensities of the two channels were scaled so that their ratio matched the ratio of integrals observed on the corresponding mass scan, and the cross sections were calculated as described by Ervin et al.[14] with a measured effective path length of 23 ± 5 cm.

Extraction of the activation energy for ligand dissociation was done with Armentrout's CRUNCH program. For the computation of the RRKM rate constant needed for the kinetic shift, frequencies

(13) Hill, G. S.; Irwin, M. J.; Levy, C. J.; Rendina, L. M.; Puddephatt, R. J. *Inorg. Synth.* **1998**, *32*, 149.

(14) Ervin, K. M.; Armentrout, P. B. *J. Chem. Phys.* **1987**, *83*, 166.

Scheme 2. Gas-Phase Synthesis and CID Reactions of 1b/c

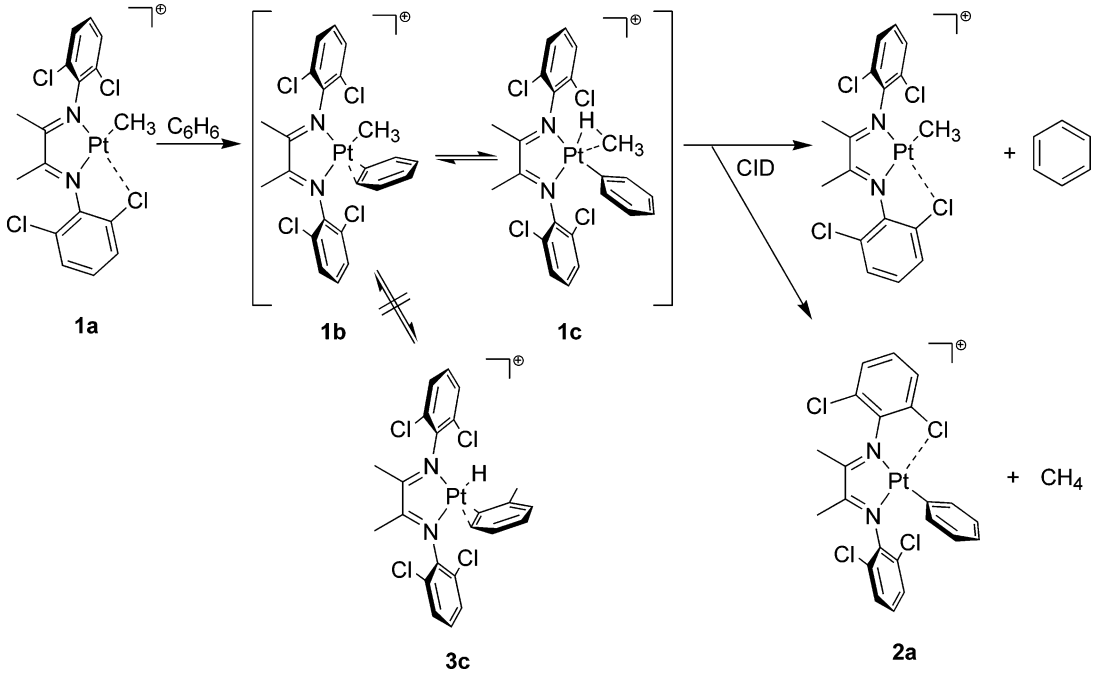

and rotational constants for both the parent molecule and the transition state are required. These were obtained from DFT calculations.

DFT Calculations. All DFT calculations were performed using Gaussian 03.[15] Geometry optimizations were performed using the Becke three-parameter hybrid functional[16] using the Perdew−Wang[17] nonlocal correlation. The Stuttgart/Dresden[18,19] basis set and effective core potential were used for Pt, along with a 6-31G-(d,p) basis set on all other atoms. All frequency calculations was performed on converged geometries and verified as minima. When convergence problems were encountered, the GDIIS[20] algorithm was used.

Transition states were computed by first performing a relaxed potential energy surface scan along a suitable coordinate and then using the highest energy point as transition state guess for the QST3 (Synchronous Transit-Guided Quasi-Newton) method[21] along with starting material and products optimized geometries. A subsequent frequency calculation was used to check that the converged geometries were first-order saddle points and that the only negative frequency corresponded to the desired reaction coordinate.

All energies were ZPE corrected using a scaling factor of 0.9774 as proposed by Scott and Radom[22] for B3PW91/6-31G(d). The drawings were made using the PLUTON module of the program suite PLATON.[23]

Results

Structure of the Adduct of 1a and Benzene. As previously reported,[12] the reaction of ion $[(N{-}N)PtCH_3]^+$ (**1a**) with benzene in the gas phase is presumed to generate the rapidly equilibrating set of ions **1b/c**, which upon CID with a rare gas loses either benzene or methane (yielding the phenyl complex **2a**), as depicted in Scheme 2. Assignment of the observed threshold for dissociation to the depicted chemical process assumes a defined structure for the ion from which the dissociation occurs. According to the Curtin−Hammet principle, the observed reaction energy in a CID threshold measurement is the energy difference between the lowest kinetically accessible minimum of the potential energy surface and the transition state leading to dissociation. So, if the studied ion would equilibrate with another structure of lower energy on the time scale of the gas-phase experiment (∼60 μs), this would result in an overestimation of the actual binding energy.

Preliminary calculations had indicated, in our case, that $[(N{-}N)PtH(C_6H_5{-}CH_3)]^+$ (**3c**) could have a lower energy than **1b/c**, while its dissociation products—namely, the cationic platinum hydride complex **3a** and toluene—could lie slightly above the observed products from dissociation of **1b/c**. This would make it possible for **3c**, if it were formed, to potentially dissociate to the same products as **1b/c**. Furthermore, as only the *m*/*z* ratio of the parent ion is measured, the hydrido toluene complex cannot be distinguished from **1b/c** in a simple mass spectrometry experiment. Thus, it was necessary to check whether they were equilibrating via a potentially

(15) Frisch, M. J.; Trucks, G. W.; Schlegel, H. B.; Scuseria, G. E.; Robb, M. A.; Cheeseman, J. R.; Montgomery, J. A., Jr.; Vreven, T.; Kudin, K. N.; Burant, J. C.; Millam, J. M.; Iyengar, S. S.; Tomasi, J.; Barone, V.; Mennucci, B.; Cossi, M.; Scalmani, G.; Rega, N.; Petersson, G. A.; Nakatsuji, H.; Hada, M.; Ehara, M.; Toyota, K.; Fukuda, R.; Hasegawa, J.; Ishida, M.; Nakajima, T.; Honda, Y.; Kitao, O.; Nakai, H.; Klene, M.; Li, X.; Knox, J. E.; Hratchian, H. P.; Cross, J. B.; Bakken, V.; Adamo, C.; Jaramillo, J.; Gomperts, R.; Stratmann, R. E.; Yazyev, O.; Austin, A. J.; Cammi, R.; Pomelli, C.; Ochterski, J. W.; Ayala, P. Y.; Morokuma, K.; Voth, G. A.; Salvador, P.; Dannenberg, J. J.; Zakrzewski, V. G.; Dapprich, S.; Daniels, A. D.; Strain, M. C.; Farkas, O.; Malick, D. K.; Rabuck, A. D.; Raghavachari, K.; Foresman, J. B.; Ortiz, J. V.; Cui, Q.; Baboul, A. G.; Clifford, S.; Cioslowski, J.; Stefanov, B. B.; Liu, G.; Liashenko, A.; Piskorz, P.; Komaromi, I.; Martin, R. L.; Fox, D. J.; Keith, T.; Al-Laham, M. A.; Peng, C. Y.; Nanayakkara, A.; Challacombe, M.; Gill, P. M. W.; Johnson, B.; Chen, W.; Wong, M. W.; Gonzalez, C.; and Pople, J. A. *Gaussian 03*, Revision C.02; Gaussian, Inc.: Wallingford, CT, 2004.
(16) Becke, A. D. *J. Chem. Phys.* **1993**, *98*, 5648.
(17) Perdew, J. P.; Burke, K.; Wang, Y. *Phys. Rev. B* **1996**, *54*, 16533.
(18) Bergner, A.; Dolg, M.; Kuechle, W.; Stoll, H.; Preuss, H. *Mol. Phys.* **1993**, *80*, 1431.
(19) Dolg, M.; Stoll, H.; Preuss, H.; Pitzer, R. M. *J. Phys. Chem* **1993**, *97*, 5852.
(20) Farkas, O.; Schlegel, H. B. *J. Chem. Phys.* **1999**, *111*, 10806.
(21) Peng, C.; Ayala, P. Y.; Schlegel, H. B.; Frisch, M. J. *J. Comput. Chem.* **1996**, *17*, 49.
(22) Scott, A. P.; Radom, L. *J. Phys. Chem.* **1996**, *100*, 16502.
(23) Spek, A. L. *J. Appl. Crystallogr.* **2003**, *36*, 7.

Scheme 3. Synthesis of (N−N)Pt(C_2H_5)$_2$ (7) and Generation of [(N−N)PtH]$^+$ (3a) in the Gas Phase

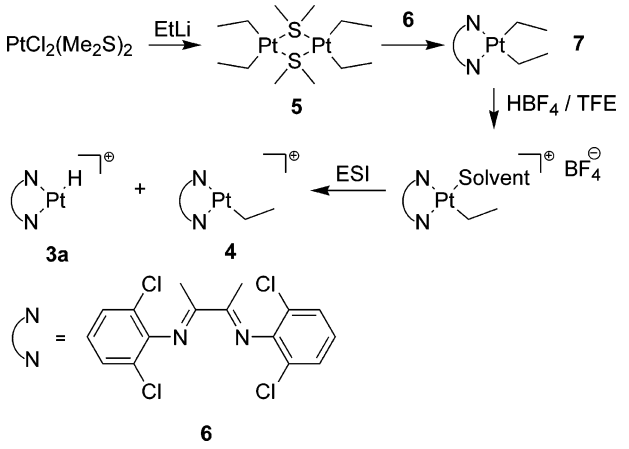

plausible reversible C−C activation reaction on the time scale of our measurements. In order to do so, **3c** was prepared from the gas-phase reaction of the hydride complex cation with toluene.

First attempts to prepare [(N−N)PtH]$^+$ (**3a**) from the reaction of **1a** with molecular hydrogen were unsuccessful. No reaction was observed in the gas phase under various conditions. In TFE solution, reaction with up to 5 bar of H_2 led only to the appearance of a peak corresponding to the known[9] decomposition ion [(N−N)Pt(CH_3)μ-OH]$_2^{2+}$ in the mass spectrum, ultimately producing Pt black.

The work of Mole et al.[24] on platinum(II) complexes with chelating diphosphines suggested to us that the desired hydride complex could be prepared by an alternative route (see Scheme 3) based on a β-hydride elimination reaction from the ethyl complex **4**. This approach proved to be successful. First, the complex $PtCl_2(SMe_2)_2$ was reacted with ethyllithium in diethyl ether at −15 °C to yield the dinuclear complex $Pt_2(C_2H_5)_4(\mu\text{-}Me_2S)_2$ (**5**). Compound **5** is a white solid that is unstable at room temperature under inert gas as well as in vacuum. It reacts with diimine **6** in diethyl ether to give the corresponding diethyl complex **7** in moderate yield. The protolysis of **7** in TFE yielded solutions from which the ethyl—or the isomeric hydrido ethylene complex (**4**)—could be electrosprayed as the most intense signal.

A ^{1}H NMR spectrum of a solution obtained by protolysis of **7** with HBF_4/H_2O in TFE-d_3 showed that at least 50% of the ions are present in the [(N−N)Pt(C_2H_5)(L)]$^+$ form. Addition of MeCN-d_3 to this solution gave one main product, which is assigned as [(N−N)Pt(C_2H_5)(CD_3CN)]$^+$, showing that no fast irreversible loss of ethylene occurs in solution at room temperature.

Collision-induced dissociation of ion **4** gave the desired hydride complex **3a** as the main ionic fragment; alternatively, tuning the tube lens potential at the entrance to the first rf-multipole to higher values generated **3a** without the need of a subsequent CID step in the collision cell.

3a was then reacted with toluene in the gas phase. Introduction of toluene in the 24-pole ion guide of our instrument, which is located before the first mass selection quadrupole, resulted in the disappearance of the peak of **3a** at m/z = 569 with concurrent appearance of a new peak corresponding to the desired toluene adduct **3c** at m/z = 661 (spectra are provided in the Supporting Information.). This product ion was then mass selected and collided with argon at a variety of pressures and collision energies, resulting only in the loss of toluene, as seen in Figure 1.

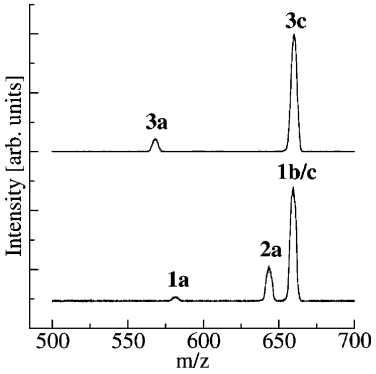

Figure 1. Daughter spectrum of **3c** (top) and **1b/c** (bottom) collided with 100 μTorr of argon at 35 V offset, showing that the parent ions do not interconvert on the measurement time scale.

Scheme 4. Reactions Studied by CID Threshold Measurements

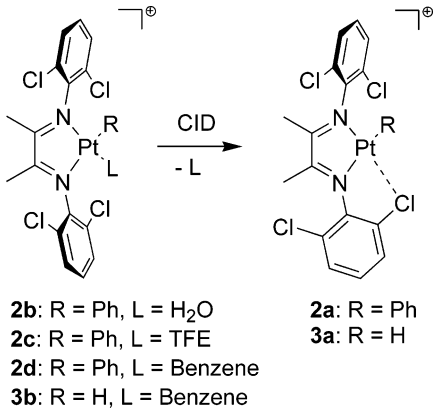

If the previously mentioned, reversible C−C activation reaction were to have taken place, the same set of fast interconverting ions would be produced from reaction of **1a** with benzene or of **3a** with toluene, and the same CID products should be observed. As is evident from Figure 1, the CID products are completely different, ruling out the possibility that the gas-phase reaction of **1a** with benzene produces the hydrido toluene complex **3c**. If one were to believe the computational prediction that **3c** represents a lower energy structure than **1b/c**, then one must postulate a high enough activation barrier for the reversible C−C activation reaction so as to render interconversion kinetically uncompetitive.

CID Threshold Measurements and DFT Calculations. Energy-resolved reactive cross-section data were acquired as described earlier[12] for the CID reactions depicted in Scheme 2 as well as for the related ions [(N−N)Pt(C_6H_5)(L)]$^+$ (L = H_2O, TFE, benzene) (**2b**−**d**) and [(N−N)PtH(C_6H_6)]$^+$ (**3b**), listed in Scheme 4.

The phenyl ions **2a**,**b** could be cleanly electrosprayed from a solution of **2b** in TFE that had been treated with benzene for ∼2 h and diluted with TFE and TFE/H_2O, respectively. The benzene adducts, **2d** and **3b**, and TFE adduct **2c** were obtained from reaction of the appropriate ions with benzene or TFE in the gas phase.

(24) Mole, L.; Spencer, J. L.; Litster, S. A.; Redhouse, A. D.; Carr, N.; Orpen, A. G. *J. Chem. Soc., Dalton Trans.* **1996**, 2315.

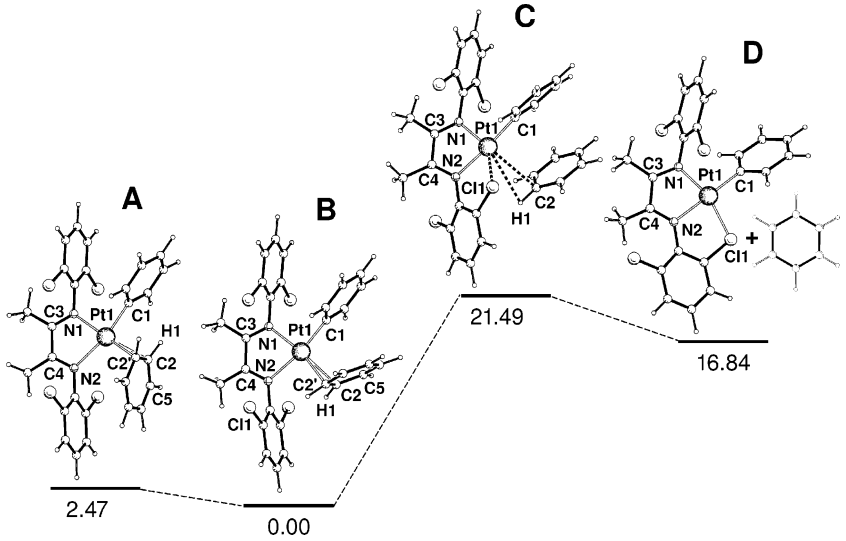

Figure 2. Calculated structures and energies [kcal/mol] for "endo" (A) and "exo" (B) **2d**, its CID products **2a** and benzene (D), and the transition state for the dissociation reaction (C). Selected distances [Å] angles [deg] and torsion angles [deg] (symmetry equivalent values are averaged): **A**: Pt1−N1 2.066, Pt1−N2 2.254, Pt1−C1 2.016, Pt1−C2 2.322, Pt1−H1 2.662; N1−Pt1−N2 74.9, N1−Pt1−C1 92.7, N2−Pt1−C2 108.4, C1−Pt1−C2 83.4; N1−C3−C4−N2 0.8, Pt1−C2′−C2−C5 110.5. **B**: Pt1−N1 2.058, Pt1−N2 2.204, Pt1−C1 2.013, Pt1−C2 2.315, Pt1−H1 2.648, Pt1−Cl1 4.164; N1−Pt1−N2 75.9, N1−Pt1−C1 94.1, N2−Pt1−C2 94.4, C1−Pt1−C2 95.1; N1−C3−C4−N2 0.5, Pt1−C2′−C2−C5 110.9. **C**: Pt1−N1 1.997, Pt1−N2 2.146, Pt1−C1 1.998, Pt1−C2 3.266, Pt1−H1 3.201, Pt1−Cl1 2.631; N1−Pt1−N2 78.0, N1−Pt1−C1 99.9, N2−Pt1−C2 90.1, N2−Pt1−Cl1 76.2; N1−C3−C4−N2 11.0. **D**: Pt1−N1 2.007, Pt1−N2 2.110, Pt1−C1 2.008, Pt1−Cl1 2.391; N1−Pt1−N2 79.1, N1−Pt1−C1 101.1, N2−Pt1−Cl1 83.6, C1−Pt1−Cl1 95.5; N1−C3−C4−N2 16.5.

Thermochemical information was extracted using the CRUNCH program,[25] which fits the dissociation cross section to eq 1:

$$\sigma(E) = \left(\frac{n\sigma_0}{E}\right) \sum_{i<\mathrm{bu}>} g_i \int_{E_0-E_i}^{E} (1 - \mathrm{e}^{-k(\epsilon+E_i)\tau})(E-\epsilon)^{n-1} d\epsilon \quad (1)$$

where E is the collision energy in the center-of-mass frame, E_0 is the reaction threshold at 0 K, σ_0 is a fitted scaling factor, n is an adjustable parameter, E_i are the energies of rovibrational states with degeneracy g_i, and k is the RRKM reaction rate with a residence time τ (estimated as 6×10^{-5} s) in the collision cell. For multiple channel fits, CRUNCH uses the following modification of eq 2:

$$\sigma_j(E) = \left(\frac{n\sigma_{0,j}}{E}\right) \sum_i g_i \int_{E_0-E_i}^{E} \frac{k_{tot}(\epsilon+E_i)}{k_j(\epsilon+E_i)} (1 - \mathrm{e}^{-k_{tot}(\epsilon+E_i)\tau})(E-\epsilon)^{n-1} d\epsilon \quad (2)$$

where $k_{\mathrm{tot}} = \sum k_j$. In the case of relatively large ions, in which vibrational energy is spread over many modes, the kinetic shift correction accounts for a large part of the observed threshold energy. Thus, an accurate computation of k, based on an appropriate transition state description, is necessary.

For simple bond dissociation reactions that proceed without a reverse barrier, the loose orbiting transition state description[26] is optimal for the treatment of the kinetic shift. In this model—the so-called phase space limit (PSL) model—the centrifugal barrier is considered as the transition state, and transitional modes are equated with rotational modes of the products. It has been used for treating a variety of metal−ligand systems,[27] including our earlier measurements of the bond dissociation energies (BDE) of solvents from cationic platinum diimine methyl complexes.[12] On the other hand, the PSL model is not appropriate for treating dissociations that go through a tight transition state, especially in the case where a reverse activation barrier exists. In this case, frequencies computed from a DFT-optimized transition structure were used when available.[28,29] Alternatively, a tight transition state can be modeled by equating the frequencies of the transition state with the ones from the parent ion, after removing the frequency that resembles most the reaction coordinate.[26]

As CRUNCH treats the kinetic shift correction without fitting any parameter to the data, additional knowledge about the nature of the transition state is needed. DFT calculations provided the necessary information. The geometries of the parent ions, **1b**,**c**, **2b**−**d**, and **3b**, and daughter ions, **1a**, **2a**, and **3a**, as well as the neutral leaving ligands, were optimized using density functional theory (DFT), using the B3PW91 exchange correlation functional[16,17] and the Stuttgart/Dresden[18,19] basis set and effective core potential for Pt with the 6-31G** basis set for all other atoms.

For the benzene complexes, **1b**, **2d**, and **3b**, two minima were found, both with an η^2 coordination mode. One of them ("exo") has the benzene ring pointing outside, in the same direction as the Pt−L bond, whereas in the other structure ("endo") the benzene ring lies parallel to the 2,6-dichlorophenyl group of the ligand. The two structures are shown in Figure 2, labeled **A** and **B**. The "exo" isomer is always found to be the more stable of the two, by 3.7, 2.5, and 4.5 kcal/mol for **1b**, **2d**, and **3b**

(25) CRUNCH, version D1, was kindly provided as an executable by Prof. P. Armentrout.

(26) Rodgers, M. T.; Ervin, K. M.; Armentrout, P. B. *J. Chem. Phys.* **1997**, *106*, 4499.

(27) Rodgers, M. T.; Armentrout, P. B. *Mass Spectrom. Rev.* **2000**, *19*, 215.

(28) Treating the reactions for which optimized transition state frequencies are available with the tight TS model based on parent ion frequencies yielded E_0 values within the experimental error.

(29) CRUNCH has been shown to be suitable for such a treatment of tight transitions states: Muntean, F.; Armentrout P. B. *J. Phys. Chem. B* **2002**, *106*, 8117.

respectively. The energetic order may be rationalized in terms of steric repulsion between the benzene ligand and the substituted phenyl group of the diimine moiety in the "endo" form, resulting in a somewhat longer Pt−N(*cis*) distance (2.25 versus 2.20 Å). However, DFT has been shown to reproduce dispersion interactions, and especially $\pi-\pi$ stacking, badly: the calculated face-to-face benzene−benzene potential energy curve is usually purely repulsive in DFT treatments, while experiment and higher level calculations show that there is an energy minimum.[30] In our case, this could lead to an overestimate of the energy of the "endo" isomers, where the benzene ligand and the diimine phenyl group are close to a face-to-face parallel configuration, and thus the energy ordering should be taken with some care. Nevertheless, Johansson et al.[10] observed that low-temperature protolysis of the related [(N^{Me}N^{Me})Pt(Me)(Ph)] (N^{Me}N^{Me} = ArN═C(Me)C(Me)═NAr, Ar = 2,6-dimethylphenyl) in dichloromethane yields a [(N^{Me}N^{Me})Pt(Me)(Benzene)]$^+$ cation in which the Pt*Me* ^{1}H NMR resonance is shielded by the ring current of the benzene ligand, giving experimental support to our finding that the "exo" conformer is more stable. These authors also observe that the two conformers interconvert quickly on the NMR time scale even at −69 °C. Thus, we assume fast equilibrium for the gas-phase reactions as well, presumably via a C−H σ complex that also lies on the C−H activation pathway, and we assume that the "exo" isomer is the ground state for the η^2-benzene complexes in further calculations and discussion.

Information about the nature of the transition states was obtained as follows. First, it was observed in all cases that, in the energy-minimized structure of the product ions of the type [(N−N)Pt(R)]$^+$, comprising **1a**, **2a**, and **3a**, the formally empty coordination site is in fact occupied by one of the *ortho* chlorine atoms of the ligand (see Figure 2, **D**). It follows that the dissociation reactions of interest should not be considered as simple bond-breaking reactions, but rather as an intramolecular associative ligand exchange reaction. Given that an associative ligand exchange occurs, in principle, through two steps, which can be more or less synchronous, and depending on which of these two steps would be actually rate-limiting, the relevant transition state for loss of a ligand could be tighter than expected for a simple dissociation. In the extreme case one could even justify a nonzero barrier for the reverse reaction.

In order to probe for the occurrence of such transition states in our diimine platinum phenyl system, relaxed structure energies were computed with decreasing, constrained Pt−Cl distances starting from the parent ion, as shown in Figure 3. In principle, one would expect a tight transition state to be found if the curve obtained this way crosses the energy of the dissociation products before the daughter ion Pt−Cl distance is reached. Interestingly this happens only in the case of the benzene and methane ligands. One can understand this by the fact that η^2-coordinated ligands fill more space in the first coordination sphere of the metal and, therefore, have to depart earlier as the incoming ligand gets closer. The existence of a reverse energy barrier for the dissociation of benzene from **1b**, **2d**, and **3b** was confirmed by optimizing a transition state geometry using the quasi-synchronous transit method.[21] A frequency calculation on these structures confirmed that only one negative frequency was present for each and that the corresponding mode consisted mainly of simultaneous shortening of the Pt−Cl and lengthening of the Pt−benzene distances,

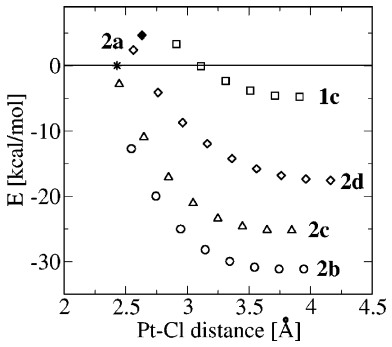

Figure 3. Relaxed PES scan along the Pt−Cl distance coordinate for [(N−N)Pt(Ph)(L)]$^+$ complexes, L = methane (squares), benzene (diamonds), TFE (triangles), and water (circles). The zero of energy is set at the energy of [(N−N)Pt(Ph)]$^+$ + L, designated by the star on the diagram. The point designated with the solid diamond represents the optimized transition state for the elimination of benzene.

Table 1. Experimental and Calculated Bond Dissociation ([Pt]$^+$ = [(N−N)Pt]$^+$, N−N = 7) (energies in kcal/mol, entropies in cal·mol^{-1}K^{-1})

fragments	TS model	$E^{\ddagger}_{0,\mathrm{exp.}}$	$\Delta S^{\ddagger}_{1000}$	$E_{0,\mathrm{DFT}}$	$\Delta E^{\ddagger}_{0,\mathrm{DFT}}$
CH_3[Pt]$^+$ + C_6H_6	tight	20.1 ± 1.7	0.5	18.3	21.5
C_6H_5[Pt]$^+$ + CH_4	tight	17.3 ± 2.1	−4.3	14.2	*a*
H[Pt]$^+$ + C_6H_6	tight	21.3 ± 1.7	−4.0	24.1	25.0
Ph[Pt]$^+$ + C_6H_6	tight	19.2 ± 1.9	0.6	16.8	21.5
Ph[Pt]$^+$ + TFE	PSL	28.4 ± 2.5	7.8	23. 6	*b*
Ph[Pt]$^+$ + H_2O	PSL	31.7 ± 2.5	6.1	28.6	*b*

[a] Transition state could not be located. [b] Calculated to be loose transition states (see Figure 3).

which suggests some synchronicity for the two formal steps in the associative ligand exchange. Unfortunately, a well-defined transition structure could not be optimized for the dissociation of methane from **1c**, presumably because the multiple binding modes of methane produce a very flat potential energy surface.

Figure 2 shows the computed structures and energies relevant to the dissociation of benzene from **2d**. The calculated transition structure is quite "product-like", as seen by the short Pt−Cl (2.63 Å) and the long Pt−C(benzene) (3.27 Å) distances and the position of the benzene molecule, which is closer to a σ-C−H coordination than to the original η^2-C−C. This is expected from the Hammond postulate for a relatively low-lying transition state (∼4.7 kcal above the products). Taking these results into account, quantitative thermochemical information was extracted from the experimental data using the tight transition state model for the benzene and methane dissociation reactions and the PSL model for the others. The results are collected in Table 1. As expected, the calculated activation entropies are largely positive for systems where the PSL model is used and small or negative for tight transition states. The uncertainty on E_0 includes contributions from the standard deviation obtained from at least three replicate data sets, a 0.15 eV (lab) uncertainty on the energy scale, and the uncertainty on the transition state model. The latter, defined as the effect of a change of $\pm R$ in the activation entropy on E_0[31] (linearly interpolated from the data fitting with the tight and loose transition state models), is the main contribution in all cases.

Agreement between calculated and experimental energies is acceptable (within ∼5 kcal) for all measurements. An extreme

(30) Sato, T.; Tsuneda, T.; Hirao, K. *J Chem. Phys.* **2005**, *123*, 104307.

(31) Wenthold, P. G. *J. Phys. Chem. A* **2000**, *104*, 5612.

case is found for the dissociation of TFE from **2c**, where the calculated energy is 4.8 kcal lower than the experimental value. This discrepancy could originate from an overestimation of the experimental value due to a partial tight character of the transition state: the relaxed PES results shown in Figure 3 indicate that the dissociation of TFE could be an intermediate case. Thus, this experimental energy should be taken with care.

Discussion

CID threshold measurement is an attractive method for obtaining thermochemical information about a variety of organometallic systems, as the involved species are often ionic and sometimes only available in very small quantities or produced *in situ*. In addition, it makes it possible to perform measurements on short-lived intermediates that are otherwise hardly accessible. The data presented here illustrate this possibility: activation energies could be measured for the dissociations of **1b/c** to **1a** and benzene and to **2a** and methane, whereas this information is usually hidden in solution-phase kinetic studies where **1b/c** are intermediates whose overall reactions are a convolution of multiple steps.

However, getting accurate information about "real life" complexes incorporating large, flexible ligands and a range of possible reactive pathways requires care with respect to several aspects. First, the nature of the observed ions should be carefully established. As mass spectroscopic methods measure the *m*/*z* ratio of the ions of interest, they cannot in general distinguish between isomers. A common way to overcome this limitation is to compare the CID patterns of ions from different preparations or reactions to assess whether they correspond to the same structure or set of equilibrating structures. We have shown here how independent synthesis and CID of a postulated ion, **3c**, could be used to rule out a possible equilibrium that would have interfered with accurate energy measurements.

Second, an increase in the size of the studied complexes implies an increased number of vibrational modes over which the deposited energy is distributed and thus slower microcanonical dissociation rates. This causes larger kinetic shift effects, for which an accurate treatment is critical. The widely used PSL model relies on the assumption that the transition state is located at the centrifugal barrier, which can be true only if no reverse activation barrier is present. While it may often be the case for simple ligand dissociation reactions, one should keep in mind that more flexible systems may offer an additional stabilization to the generated free coordination site, resulting in more complex intramolecular associative substitution pathways. Such reactions can exhibit a reverse activation barrier, making the PSL model inappropriate, as found in the case of benzene and methane dissociation reactions. The naive assumption that for similar ions an inaccurate treatment of the kinetic shift would result only in a systematic error—still yielding relevant relative energies—would have been wrong in the case of the $[(N-N)Pt(Ph)(L)]^+$ series (**2b**−**d**). The expected binding energy sequence (benzene < TFE < water), consistently supported by our DFT calculations (see Table 1) and solution-phase observations,[10] would not be obtained using a single transition state model (see Table 2). On the other hand, our differentiated treatment based on *ab initio* calculations does reproduce this sequence.[32]

Table 2. Comparison of the PSL and Tight Transition State Models (energies in kcal/mol, entropies in cal·mol^{-1}K^{-1})

	PSL		tight	
fragments	$\Delta E^{\ddagger}_0$	$\Delta S^{\ddagger}_{1000}$	$\Delta E^{\ddagger}_0$	$\Delta S^{\ddagger}_{1000}$
$CH_3[Pt]^+ + C_6H_6$	29.5	12.0	20.1	0.5
$C_6H_5[Pt]^+ + CH_4$	26.2	4.4	17.3	−4.3
$H[Pt]^+ + C_6H_6$	33.6	10.8	21.3	−4.0
$Ph[Pt]^+ + C_6H_6$	29.4	11.7	19.2	0.6
$Ph[Pt]^+ +$ TFE	28.4	7.8	17.6	−2.8
$Ph[Pt]^+ + H_2O$	31.7	6.1	20.6	−3.1

One may argue that, if the dissociation of the benzene adducts **1b/c**, **2d**, and **3b** were to proceed through a tight transition state, implying a reverse activation barrier, it might be reasoned that the complexes should hardly form at all in the gas phase because of that same barrier. It would present a problem in our experiment where we use the reverse reaction to synthetize these ions in the gas phase. Consideration of two aspects solves this apparent contradiction. First, the postulated tight transition states have a relatively small enthalpic barrier (less than 5 kcal/mol according to DFT as shown in Table 1), but exert their effect on the kinetic shift correction through the higher frequencies. Second, under the conditions used in the gas-phase ion−molecule preparation of the ions (24-pole ion guide without an external longitudinal potential, 3−10 mTorr benzene), the ions undergo a high number of collisions ($\gg 10^4$ according to Monte Carlo simulations as described in ref 33). Both considerations combine to allow the gas-phase synthesis to proceed even if the reaction under single-collision conditions would have a low probability due to an activation barrier.

The energies shown in Table 1 are activation energies for the observed dissociations, which can be interpreted as actual binding energies only in the case of water and TFE departure where no reverse activation barrier is present. In both cases, they can be seen as an estimate of the activation energy for formally dissociative ligand exchange in solution, assuming small enough medium effects. In contrast, ligand exchange is usually an associative process in square planar Pt complexes and has been shown to be associative in the case of acetonitrile for complexes closely related to **1** and **2**. Thus, these values give an approximate upper bound to the range of possible activation energies for associative ligand exchange.

The *ortho* chlorine substituent in the diimine ligand has been found here to assist the departure of the leaving group and stabilize the free cation. In the case of related Pt(II) complexes in which the *ortho* position on the aryl substituent is occupied by a methyl group instead of a chlorine, we had previously observed isotope exchange on the methyl group when the complex was reacted with C_6D_6. We interpreted the observation to indicate that a reversible, intramolecular C−H activation had occurred, which necessarily implies that a precursor C−H complex, which suggests in turn that the chlorine substituent in **1** and **2** is not unique in its ability to fill the nominally empty coordination site on Pt.

(32) An interesting example of a system that can be treated appropriately only by considering both tight and loose transition states for different channels can be found in: Muntean, F.; Armentrout P. B. *Z. Phys. Chem.* **2000**, *214*, 1035.

(33) Adlhart C.; Hinderling C.; Baumann H.; Chen P. *J. Am. Chem. Soc.* **2000**, *122*, 8204.

Conclusions

Quantitative thermochemical information was obtained for species appearing on the potential energy surface of a C−H activation reaction via CID threshold measurements. Accurate modeling of the transition states for ligand dissociation is critical for obtaining reliable data, and DFT calculations were used for this purpose. In particular, the dissociation reactions were found to be best described as intramolecular associative ligand exchange processes, exhibiting tight transition states in the cases of η^2-coordinating hydrocarbon ligands. The results are in good agreement with computed DFT energies, as well as with qualitative solution-phase observations.

Acknowledgment. The authors acknowledge support from the Swiss National Science Foundation and the Research Commission of the ETH Zürich.

Supporting Information Available: Mass spectra showing the gas-phase synthesis of **3c**; energy-resolved CID cross-section data and fitting; optimized structures, harmonic frequencies, rotational constants, and energy of all calculated minima and transition states.

OM0610039